Al-Azhar University Civil Engineering Research Magazine (CERM)
Vol. (39) No. (3) july, 2017

CONTRIBUTION OF INNER STIRRUPS WITH THE HANGER STEEL OF LEDGE BEAM

Prof. Dr. Ayman Hussein[1], Dr. Mohamed Nabil[2], Dr. Ezz El-Deen Mostafa[2] and Eng. Yasser EL Sayed EL Badawy[3]

Structural Engineering Department, Faculty of Engineering, Ain Shams University, Cairo, Egypt

1. *Professor of R.C. structures*
2. *Ass. Professor, Structural Engineering Department*
3. *Structural Engineer,* Engineering for the Petroleum and Process Industries *Engineering Department*

ملخص البحث

الكمرات ذات القطاع على شكل "L" تستخدم عادة ككمرات حاملة للمنشآت الخرسانية سابقة الصب . تصميم هذه الكمرات طبقا للكود الأمريكي يفترض أن الأفرع الخارجية للكانات الرأسية هي التي تقاوم الاجهادات الناتجة عن عزوم الالتواء وكذلك تعمل هذه الأفرع الخارجية كشداد لحمل الجزء السفلي من الكمرة . عمل الأفرع الداخلية للكانات الرأسية كشداد يتم إهمالها في التصميم لذلك فإن الأفرع الخارجية تكون ذات أقطار كبيرة بالنسبة للأفرع الداخلية . يعتمد البرنامج العملي على دراسة مقدار مساهمة الأفرع الداخلية للكانات في العمل كشداد لحمل الجزء السفلي من الكمرة . تتكون العينات من عدد 4 كمرات بسيطة الارتكاز تبلغ بحورها الفعاله 2700 مم. جميع هذه الكمرات لها ارتفاع ثابت هو 380مم وعرض جزع الكمرات 250مم وارتفاع الجزء السفلي من الكمرة "Ledge" يبلغ 140مم بعرض ثابت قدره 300 مم . المتغير الأساسي في هذه العينات هو توزيع الأفرع الرأسية للكانات الداخليه في القطاع .تم تصميم هذه الكمرات بحيث نضمن ان انهيار الجزء السفلي من الكمرة"Ledge" يحدث قبل انهيار الكمرة بالانحناء أو القص .

ABSTRACT

Ledge beams are commonly used as spandrels in precast concrete structures. The design of ledge beams according to the ACI code [1] and PCI [9] assumes that the outer branches of vertical stirrups are resisting torsion stress and acting as a hanger for the ledge part. The contribution of the inner vertical branches of stirrups as a hanger for the ledge part is neglected. Therefore, the outer vertical stirrups have a great amount of reinforcement with respect to the internal stirrups.

This paper aims to study the contribution of the internal vertical stirrups on the hanging action of the ledge. The experimental program consist of testing four simply supported RC beams with effective span 2700 mm. All beams have a total height of 380 mm and a web width of 250 mm. The heights of the ledge part were 140 mm and their projection was 300 mm. The studied main variables are the distribution of internal vertical stirrups and the eccentricity of vertical loads. The specimens were designed to ensure that the ultimate failure load of the ledge part due to yielding of the vertical hanger outer stirrups according to the ACI code [1] and PCI [9] was smaller than the ultimate flexural and punching shear failure loads of the specimens.

To evaluate the results of the experimental program, a finite element program will be used to simulate the beams by using the computer program. A comparison between the obtained results of this research and code equations will be achieved to improve the analysis methods of ledge beams.

Key Words: Shear friction, Shear reinforcement, Ledge beam & Reinforced concrete.

1. INTRODUCTION

The design of ledge RC beams, commonly used as spandrels in precast concrete structures, may not be adequate under currently accepted criteria based on the ACI code [1] and the PCI Design Handbook [9]. That is because the actual behavior between the ledge part and the web part of the beam must be investigated. The current design procedure recommended by PCI Design Handbook [9] and ACI code [1] assumes that the outer branches of vertical stirrups are resisting torsion stress and acting as a hanger for the ledge. The contribution of the internal vertical branches of stirrups as a hanger for the ledge is neglected which is questionable. Therefore, the outer vertical stirrups have a great amount of reinforcement with respect to the internal stirrups. Also, the punching shear behavior of the ledge part must be considered to understand the load transfer from the ledge to the beam web. The failure of ledge part has many reasons such as bearing failure under loading plates, shear friction failure, flexural failure and punching failure.

The scope of this work can be summarized as follow:

a) Studying the effect of inner stirrups distribution on the hanging behavior of ledge part.

b) Studying the effect of inner stirrups distribution on the hanging behavior of ledge part.

c) Investigating the shape of failure and its reason.

d) Making a final conclusion based on the results obtained from the experimental and numerical studies.

2. EXPERIMENTAL PROGRAM

2.1. Details of RC. Tested Beams

The experimental program consists of testing four simply supported RC ledge beams (A1, A2, A3, and A4) which tested under concentrated single load at mid-span. The beams were 380 mm total height, 250 mm web thickness and 140 mm ledge thickness. As shown in Figures 1, 2, 3 and 4, In addition, the properties of each beam are summarized as follows:

Beam A1: This beam was designed to serve as a control specimen for the testing program. The web stirrups consisted of external closed stirrups of rebar of 8 mm diameter with 200 mm spacing. The ledge part reinforcement consisted of closed stirrups of rebar of 12 mm diameter with 100 mm spacing. The top longitudinal reinforcement of the web, intermediate and bottom longitudinal reinforcement of the ledge part consisted of Rebar of 12 mm diameter. The bottom longitudinal reinforcement of the web consisted of rebar of 16 mm diameter. The stirrups are tied well to both top and bottom longitudinal steel reinforcement.

Beam A2, A3 and A4: The beams had the same geometry and reinforcement configuration of beam A1. The only difference is that using of inner stirrups for the web part of 8 mm diameter with 200 mm spacing and spaced 40 mm, 70 mm and 100 mm from the hanger steel reinforcement bar for A2, A3 and A4 respectively.

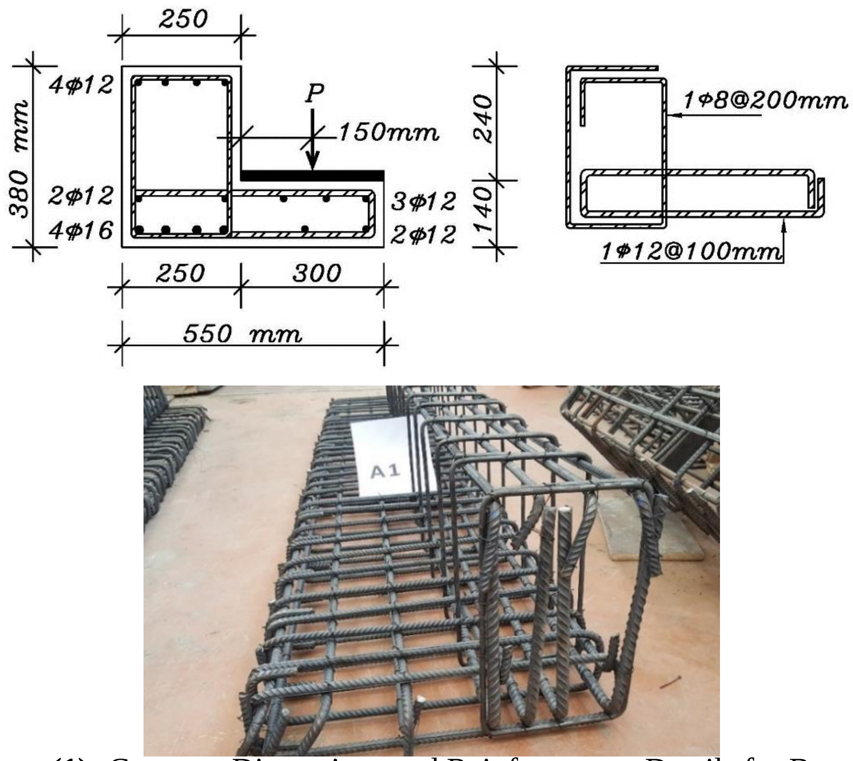

Figure (1): Concrete Dimensions and Reinforcement Details for Beam (A1)

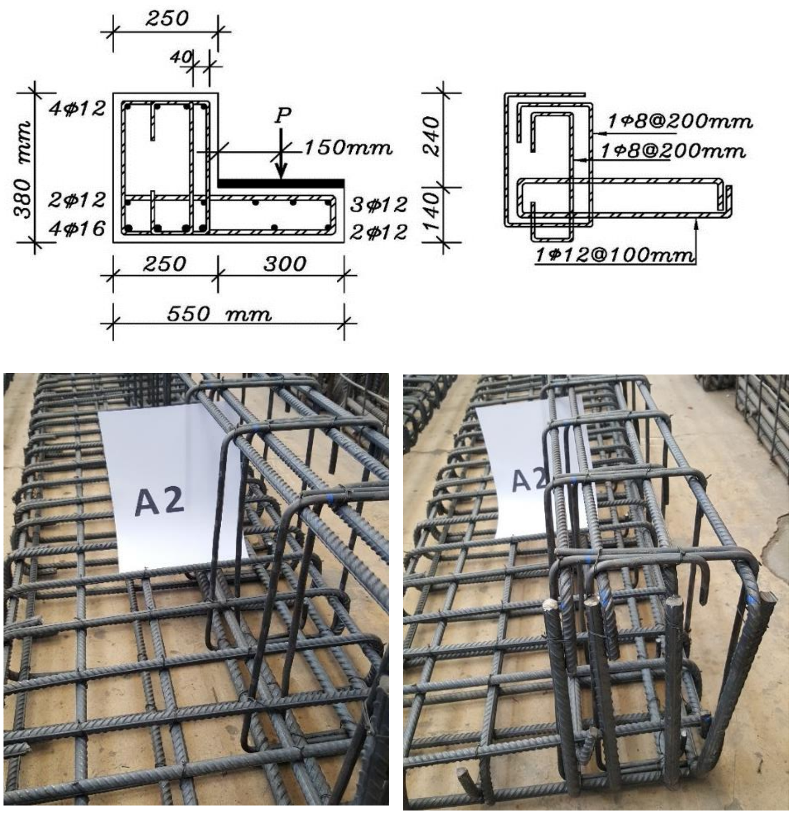

Figure (2): Concrete Dimensions and Reinforcement Details for Beam (A2)

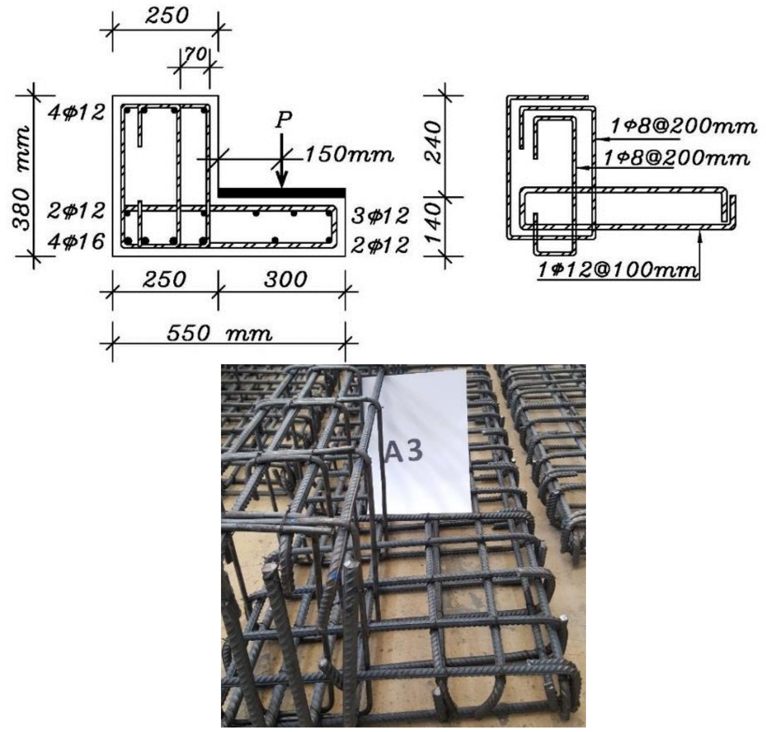

Figure (3): Concrete Dimensions and Reinforcement Details for Beam (A3)

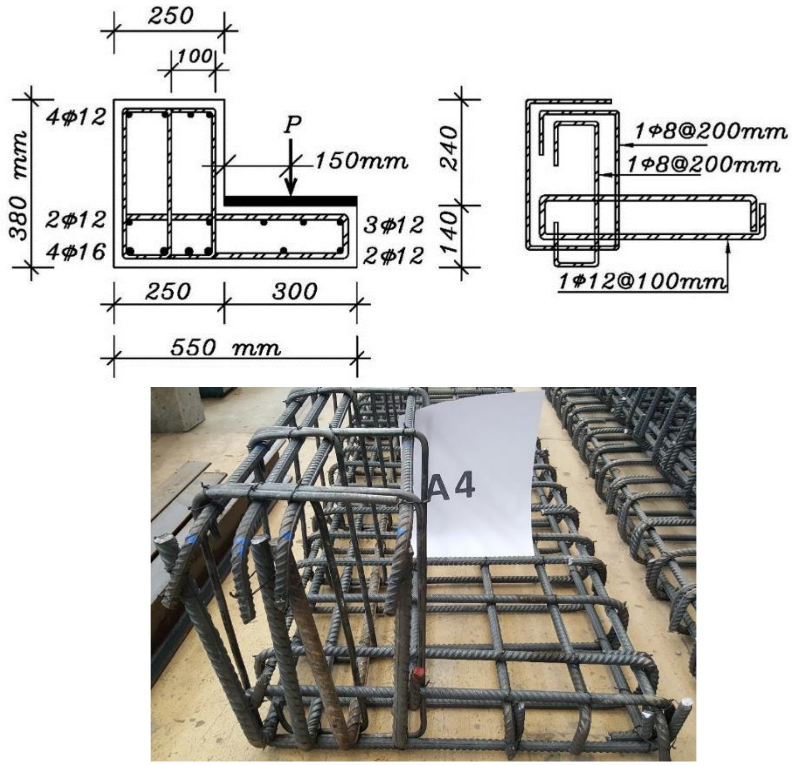

Figure (4): Concrete Dimensions and Reinforcement Details for Beam (A4)

2.2. Material Properties

2.2.1. Concrete

The concrete used was made of a mix of natural sand, natural well graded gravel, ordinary Portland cement and tap water. Mix properties, by weight, used for tested specimens are shown in Table 1**.** The concrete used was a normal weight concrete with characteristic compressive concrete strength 30 Mpa.

Table (1): Mix properties for the used concrete mix (by weight)

Cement (kg)	**Sand (kg)**	**Gravel (kg)**	**Water (kg)**
405	685	1120	190

2.2.2. Steel Reinforcement

Locally manufactured mild steel smooth bars was used for rebar of 8 mm diameter, the high tensile deformed steel bars was used for rebar of 12 mm and 16 mm diameter. Tension test was carried out for each different bar diameter. The test results shown that the rebar of 8 mm diameter have a minimum yield stress of 300 MPa and a tensile strength of 475 MPa, the rebar of 12 mm diameter have a minimum yield stress of 375 MPa and a tensile strength of 550 MPa and the rebar of 16 mm diameter have a minimum yield stress of 470 MPa and a tensile strength of 650 MPa, respectively.

2.3. Test Setup and Instruments

The tested beams were simply supported vertically using steel plates rested above rigid concrete blocks and tied horizontally to steel beam of testing frame at the ends. The holes in the spandrel beam web were aligned with the holes in the steel beam, two threaded rods at each side passed through to tie the spandrel laterally in the steel beam and to prevent the spandrel from tipping over. Steel plates of 300 x 400 x 25 mm were used as a packing plate between the spandrel web and the steel beam at the lateral fixation locations to allow the rotation of the spandrel beam, Figure 5 and 6 shown the sketch and the actual test setup respectively.

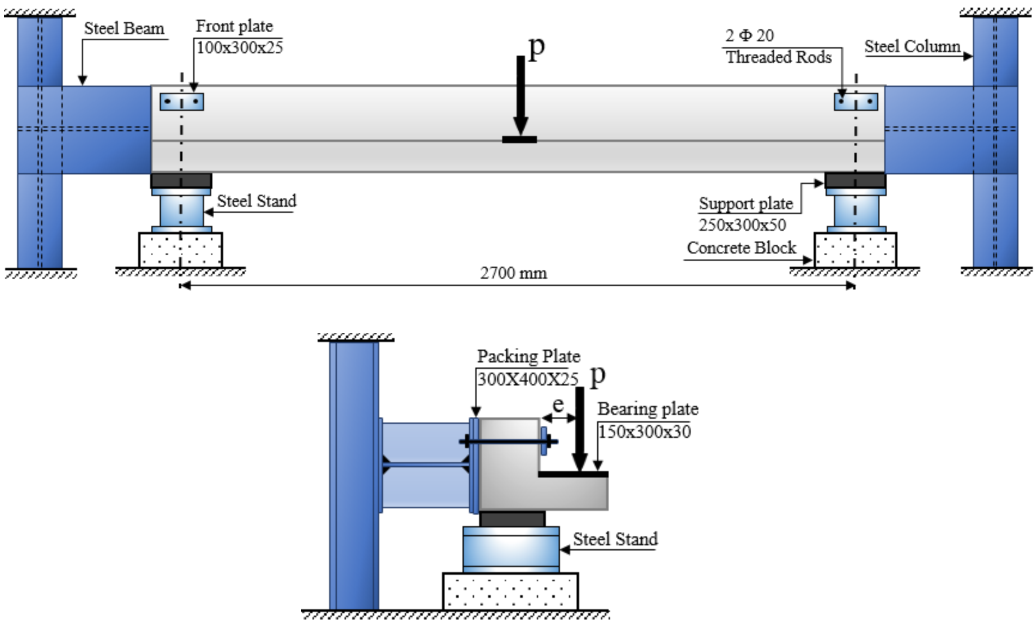

Figure (5): Loading setup for tested beams

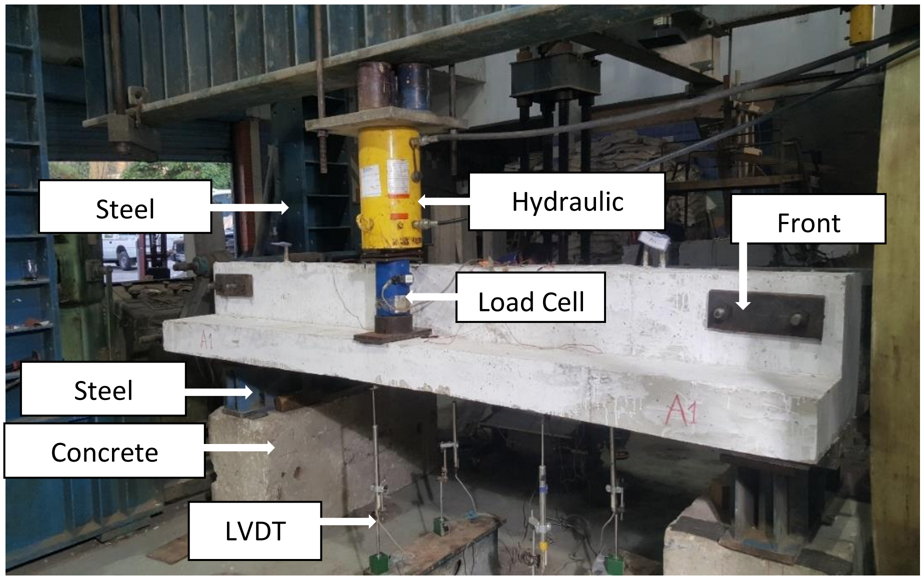

Figure (6): Test setup

2.3.1. Test Procedure

The load was applied to the ledge by the Hydraulic jacks and load cell was used to measure the applied load. A rigid steel plate of 150 mm x 300 mm x 25 mm was used to distribute the applied load uniformly onto the ledge. The vertical load is acting eccentric at 150 mm distance apart from the inner face of beam web for beams from A1 to A4 as shown in Figure 7.

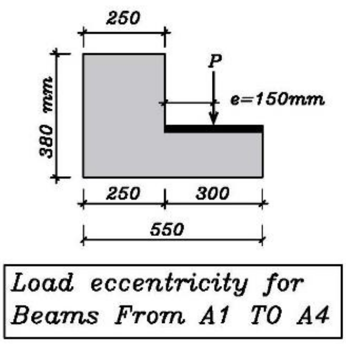

Figure (7): Load eccentricity for specimens

2.3.2. Measuring Devices

Concrete and steel strains were measured using electrical strain gauge with 120 ohm resistance fixed on the extreme compression fiber and steel bars. These gauges were fixed on the steel bars before casting, using special glue, and then covered with a water proofing material to protect them. Locations of strain gauges and deflectometers are shown in Figures 8 & 9, respectively.

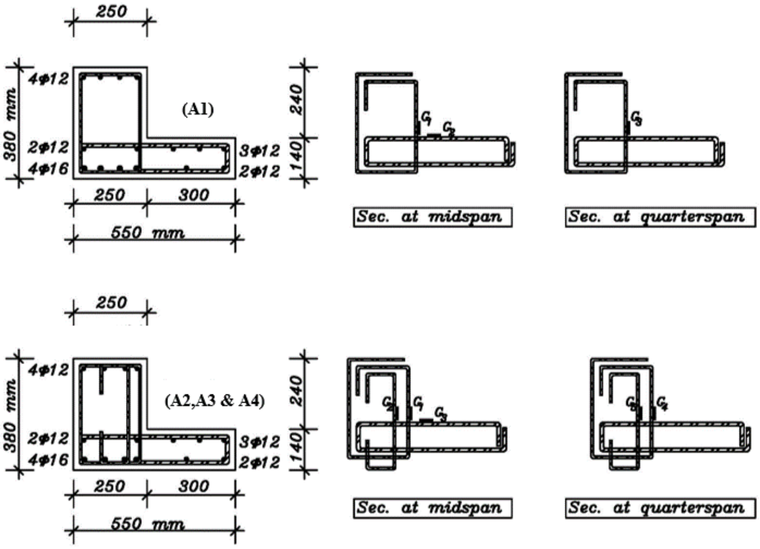

Figure (8): Locations of steel strain gauges for tested beams

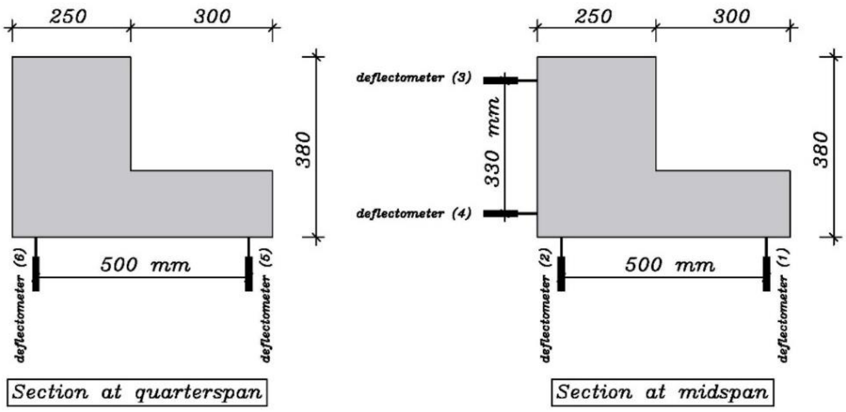

Figure (9): Location s of deflectometers for tested beams

3. EXPERMENTAL RESULTS

3.1 Crack Patterns, Cracking Loads and Failure Loads

The observed behavior under the applied concentrated load for the tested ledges indicated that the first crack was a longitudinal crack initiated at the ledge and web junction. As the load was increased, the width of these cracks become wider and extended along the length of the beam and propagated horizontally with an angle into the front face of the ledge. Prior to punching failure, additional cracks were initiated at the back of the bearing plate and extended diagonally to the horizontal surface of the ledge. Finally punching failure occurred by sudden initiation of vertical diagonal cracks of the ledge, as shown in Figure 11.

Table 2 shown that the hanger failure load calculated by PCI Design Handbook [9] for the beams A1 (control beam) is compatible with the experimental results which indicate a good agreement with the PCI design equation of the hanger steel reinforcement, on the contrary the hanger failure load calculated by "PCA Notes" equation is much smaller than the calculated by the PCI equation , this is attributed to the fact that the effective width of hanger steel calculated by "PCA Notes" is smaller than the effective width calculated by PCI.

PCI hanger steel capacity equation doesn't consider the participation of inner stirrups in the hanger load calculation, thus an assumption that the inner stirrups will contribute with the external hanger with the same full effective width as the external stirrups $(w_b + 12h_l)$ by substituting in Equation (1), which modified from PCI equation to consider the inner stirrups participation,

$$\left[(A_{sh(ext)}f_{y(ext)}\mathrm{d}_{s(ext)} + A_{sh(inner)}f_{y(inner)}\mathrm{d}_{s(inner)}\right] * \frac{(w_b+12h_l)}{s} = V_u\left[(d) - \left(3 - \frac{2h_l}{h}\right)\left(\frac{h_l}{h}\right)^2\left(\frac{b_l}{2}\right) - e\gamma_t\,\frac{(x^2y)_l}{\sum x^2y}\right] \quad \text{(Eq.1)}$$

As the calculated hanger failure load (shown in the third column of table 2) using Equation (1) are much more than the obtained experimental hanger failure load results (shown in the second column of table 2), this is indicated that the actual inner stirrups effective width shall be less than $(w_b + 12h_l)$, so a modified Equation (2) are proposed to calculate the hanger failure load as shown in Figure 10.

The actual effective width $(w_b + B_{ei}h_l)$ was calculated by getting the factor (B_{ei}) shown in the fifth column of Table 2 which had been calculated by substituting with the experimental hanger failure load (V_u) in Equation (2)

$$\left[(A_{sh(ext)}f_{y(ext)}\mathrm{d}_{s(ext)} * \frac{(w_b+12h_l)}{s} + A_{sh(inner)}f_{y(inner)}\mathrm{d}_{s(inner)} * \frac{(w_b+B_{ei}h_l)}{s}\right] = V_u\left[(d) - \left(3 - \frac{2h_l}{h}\right)\left(\frac{h_l}{h}\right)^2\left(\frac{b_l}{2}\right) - e\gamma_t\,\frac{(x^2y)_l}{\sum x^2y}\right] \quad \text{(Eq.2)}$$

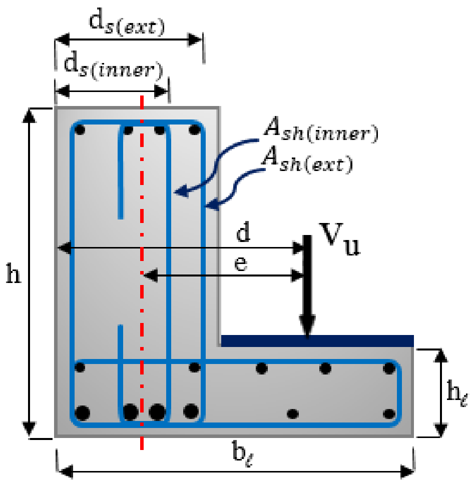

Figure (10): Design of hanger steel reinforcement

Where;

V_u = hanger failure load

$A_{sh(ext)}$ = external stirrups hanger steel area.

$f_{y(ext)}$ = yield strength of external stirrups hanger reinforcement.

$d_{s(ext)}$ = distance measured from external stirrups to the outer web side.

$A_{sh(inner)}$ = inner stirrups hanger steel area.

$f_{y(inner)}$ = yield strength of inner stirrups hanger reinforcement.

$d_{s(inner)}$ = distance measured from inner stirrups to the outer web side.

w_b = bearing plate width

S = spacing between stirrups

B_{ei} = effective width factor which calculated based on the experimental results.

x, y = shorter and longer sides, respectively, of the component rectangles forming the ledge and the web parts of the beam.

γ_t = 0, when closed ties are not used in the ledge.

γ_t = 1, when closed ties are used in the ledge.

Table 3 shows that the punching failure load calculated using PCA equation are compatible with the experimental results which indicate a good agreement with the PCA punching design equation, on the contrary the punching failure load calculated by PCI is smaller than the calculated by the "PCA Notes" and this is attributed to the fact that critical perimeter for punching shear design of PCA are greater than of PCI perimeter.

In addition, Table 3 shows that the calculated punching load capacity calculated by PCA had a lower value than the experimental punching load failure that load eccentricity doesn't considered in the PCA design equation.

A summary of the obtained experimental results are shown in Table 2, 3 and 4.

Table (2): Experimental cracking and hanger failure loads versus the PCI and ACI code

Specimen	Exp. cracking load (kN)	Exp. Hanger failure load (kN)	PCI Hanger failure load (kN)	PCA Hanger failure load (kN)	$\%\left(\frac{Exp}{PCI}\right)$	B_{ei} Effective width factor	Parameter Tested
A1	90	125	120	45	104	N/A	Control Beam
A2	105	146	218	90	67	2.40	(Inner stirrups spaced 40 mm)
A3	91	135	202	90	67	1.40	(Inner stirrups spaced 70 mm)
A4	90	129	186	90	69	0.80	(Inner stirrups spaced 100 mm)

Table (3): Experimental punching failure loads versus the PCI and ACI

Specimen	Exp. Punching failure load (kN)	PCI Punching failure load (kN)	PCA Punching failure load (kN)	$\% \left(\frac{Exp}{PCI}\right)$	$\% \left(\frac{Exp}{PCA}\right)$	Parameter Tested
A1	197	144	206	136	95	Control Beam
A2	209	144	206	145	101	(Inner stirrups spaced 40 mm)
A3	227	144	206	157	110	(Inner stirrups spaced 70 mm)
A4	218	144	206	151	106	(Inner stirrups spaced 100 mm)

Table (4): Experimental test results for all specimens

Specimen	Maximum Ledge deflection at failure load (mm)	Maximum outer deflection at failure load (mm)	Inner stirrup strain at mid span (□□)at the hanger failure load*10^{-6}	Parameter Tested
A1	39	8.5	N/A	Control Beam
A2	39	10.0	1968	(Inner stirrups spaced 40 mm)
A3	35	12.0	1300	(Inner stirrups spaced 70 mm)
A4	35	11.0	830	(Inner stirrups spaced 100 mm)

(a) Cracking pattern of the hanger steel failure

(b) Propagation of the cracks on front of the ledge

(c) Cracking pattern of punching failure

Figure (11): Crack patterns and failure shape for beam A1,

Other results can be found elsewhere [12]

3.2. Deformation of Tested Beams

The deformations for all tested specimens that include vertical and lateral deflections at specified locations will be discussed here. Deformations are recorded with load increment and up-till specimens' failure.

The load - vertical deflection behaviour of tested beams A2, A3 and A4 are compared with beam A1 (control beam) as shown in Figure 12, 13 and 14, respectively. String potentiometers placed along the web face (inner deflection side) and ledge (outer deflection side) at both mid and quad span to measure the vertical deflection. The deflection behaviour at the selected locations indicates that the maximum deflection occurred at the ledge of the beam due to the load eccentricity.

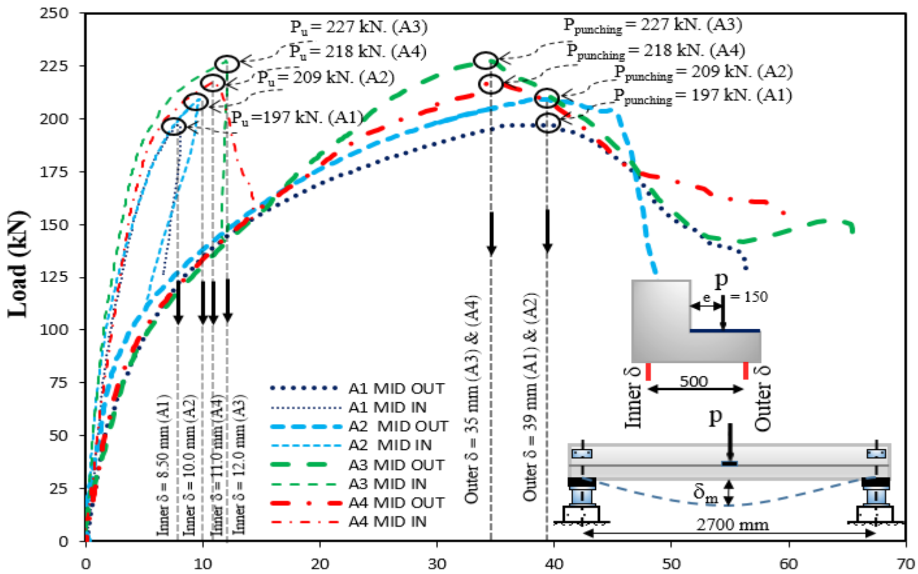

Figure (12): Load versus mid-span vertical deflection of beams A1 to A4

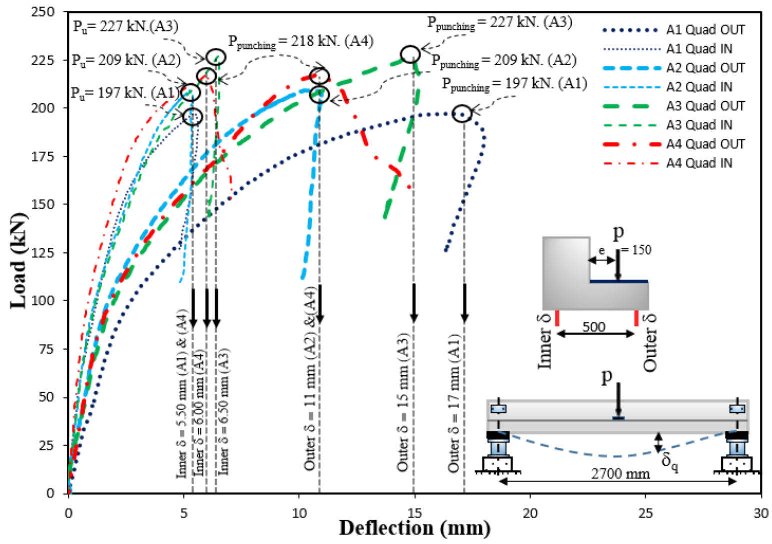

Figure (13): Load versus quad-span vertical deflection of beams A1 to A4

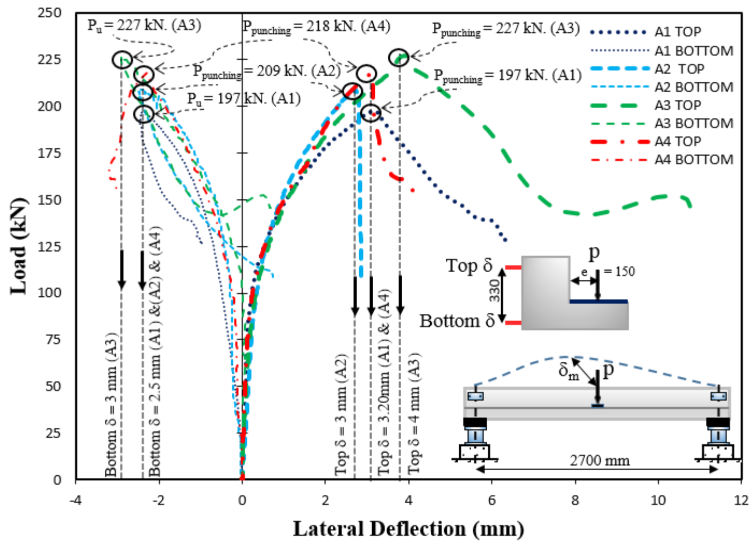

Figure (14): Load versus mid-span lateral deflection of beams A1 to A4

From these figures, it can be concluded that the inner stirrups participate and affect the torsion rigidity of the section. The specimens (A2, A3 and A4) which had the inner stirrups so, it had the minimum vertical and lateral deflection compared to specimens (A1) which with no inner stirrups. The test results had shown that there was a contribution of the inner stirrups on the hanging behaviour of the ledge part. It must be noticed that the failure load had increased due to the distribution of the inner stirrups.

3.3 Strain of Steel Stirrups of Tested Specimens

3.3.1 Control Specimen (Beam A1)

The obtained results of the load-strain curve for the outer stirrups (hanger steel reinforcement) at mid-span (□□) for beam A1 are shown in Figure 15.

The recorded yield load of the hanger steel reinforcement for beam A1 is 125 kN as shown in Figure 15, which indicated that the PCI equation of calculating the hanger steel capacity is very realistic, where the theoretical hanger failure load was 120 kN as shown in Table 2.

The results of the load-strain curve for the outer stirrups at quad-span ($\square_{\square}$) for beam A1 are shown in Figure 17.The recorded strains (ε_3) at the yield load value (125 kN) was equal to 170 με which was too small than the stirrups yield strain value (2000 με) that indicated a good agreement with using the PCI effective width equation $(w_b + 12h_l)$ to consider that all hanger stirrups are effective within this width as shown in Figure 17. In addition, it was observed that the stirrups at quad span reached to the yield strain value before the final punching failure load (197 kN) as shown in Figure 17.

3.3.2 Effect of inner stirrups (Beams A2, A3 and A4)

Tested beams A2, A3 and A4 had the same concrete dimensions and steel reinforcement details similar beam A1, but with an additional inner stirrups row with a different distance between the outer and inner stirrups branches.

The load-strain behaviour of outer and inner stirrups at mid and quad span for all beams A2, A3 and A4 are shown in Figures 15, 16, 17 and 18.

The results of the load-strain curve for the outer stirrups (hanger steel reinforcement) at mid-span ($\square_{\square}$) are shown in Figure 15. Moreover, Figure 15 indicated that the strain in the outer stirrups branches at mid-span ($\square_{\square}$) for beams A2, A3 and A4 was decreased at the same failure load of A1 which is 125 kN, and the steel hanger failure load values was increased by reducing the distance between the outer and inner stirrups branches which indicated the participation of the inner stirrups branches with the outer stirrups hangers. The recorded yield load of the hanger steel reinforcement for beams A2, A3 and A4 is 146 kN, 135 kN and 129 kN respectively as shown in Figure 15, which indicated the contribution of the inner stirrups branches by increasing the final hanger steel capacity, as adding one row of inner stirrups spaced 40 mm, 70 mm, 100 mm respectively from the main outer stirrups hangers increased the stirrups hanger failure yield load by 17 %, 8% and 3 % respectively. In addition, It was observed that the hanger failure load for A2, A3 and A4 was smaller than the expected calculated hanger failure load by PCI [9] shown in Table 2, that the hanger failure load calculated by PCI [9] was based on the assumption that the inner stirrups contributed with the outer stirrups hanger with the same effective width $(w_b + 12h_l)$,whereas the obtained experimental results indicated that the effective width $(w_b + B_{ei}\, h_l)$ for the inner stirrups was less than the proposed assumption, the calculated B_{ei} value for A2, A3 and A4 was 2.40, 1.40 and 0.80 instead of 12 respectively.

The results of the load-strain curves for the inner stirrups at mid - span ($\square_{\square}$) are shown in Figure 16, which indicated that strain in inner stirrups was increased by reducing the distance between the outer and inner stirrups branches which mean that the participation of inner stirrups was increased by reducing the distance between the outer and inner stirrups branches.

The results of the load-strain curves for the outer stirrups at quad - span ($\square_{\square}$) are shown in Figure 17, the test results of steel strain in stirrups shown that strain in outer stirrups was decreased by reducing the distance between the outer and inner stirrups branches at the same load. Moreover, it was observed that the steel strain of outer stirrups at quad - span were small and didn't reach to the yield at the hanger failure load as shown in Figure 17. In addition, the strain of outer stirrups for A2 and A3 didn't reach to the yield until the punching failure load while for A4 had been reached to the yield before the punching failure load as the behaviour of beam A1 which confirmed that increasing the distance between the outer and inner stirrups may made the increasing of the hanger load capacity is negligible.

The results of the load-strain curves for the inner stirrups at quad-span are (□□) shown in Figure 18, the test results of steel strain in stirrups for beams A2, A3 and A4 shown that small difference in the strain of inner stirrups until the hanger failure load which mean that the effective width of inner stirrups didn't extend to the quad-span.

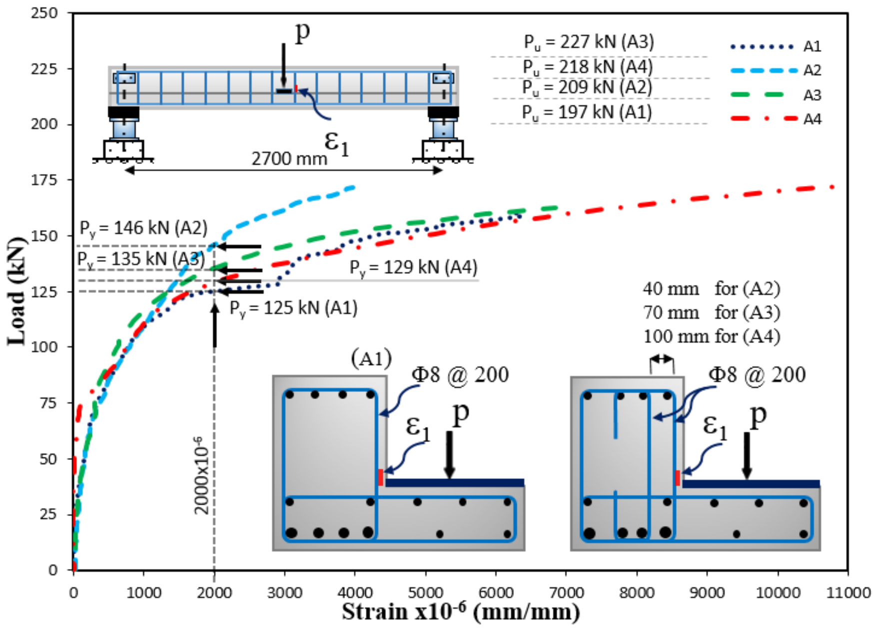

Figure (15): Load versus strains of outer stirrups (□□) at mid-span of beams A1 to A4

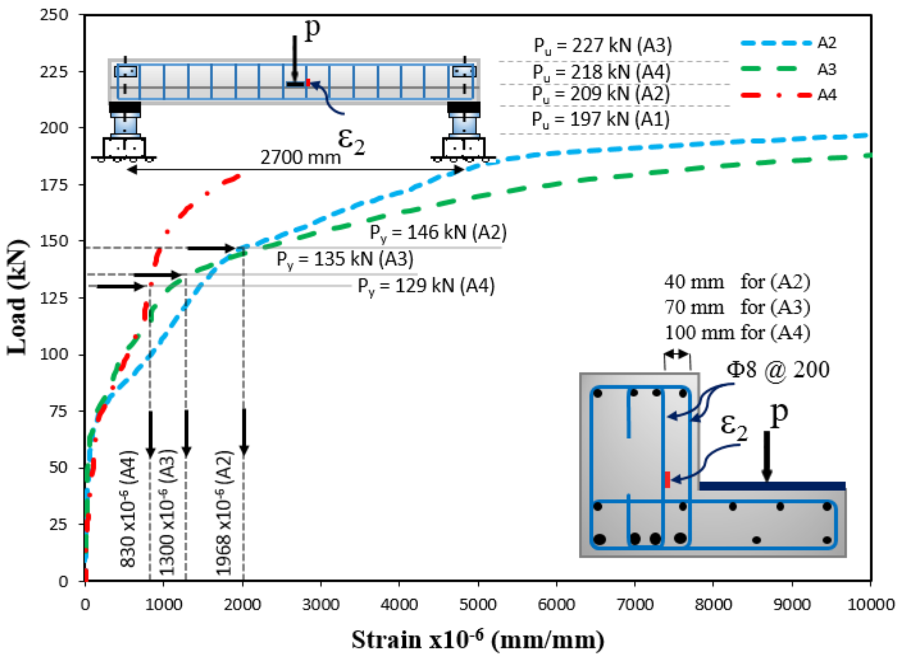

Figure (16): Load versus strains of inner stirrups (□□) at mid-span of beams A1 to A4

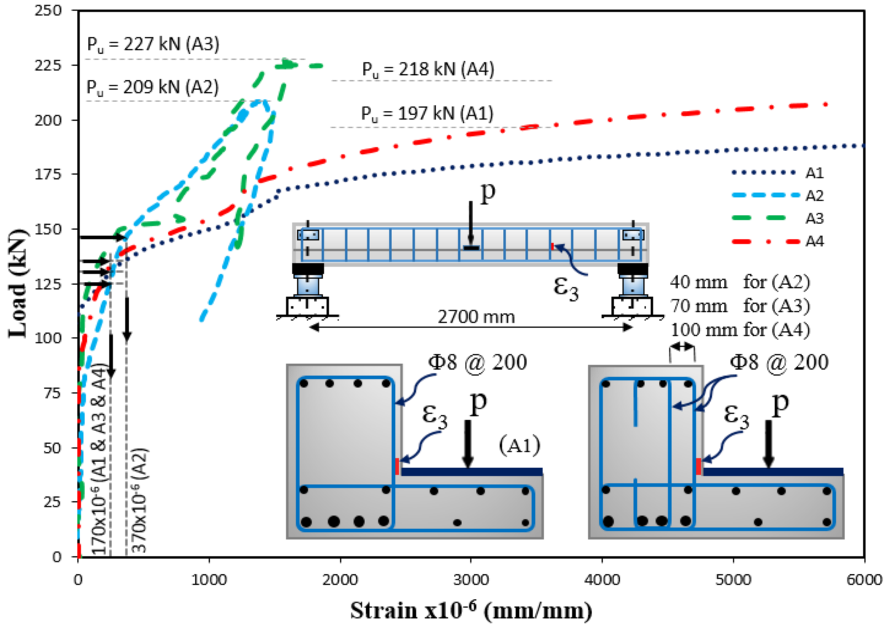

Figure (17): Load versus strains of outer stirrups (□□) at quad-span of beams A1 to A4

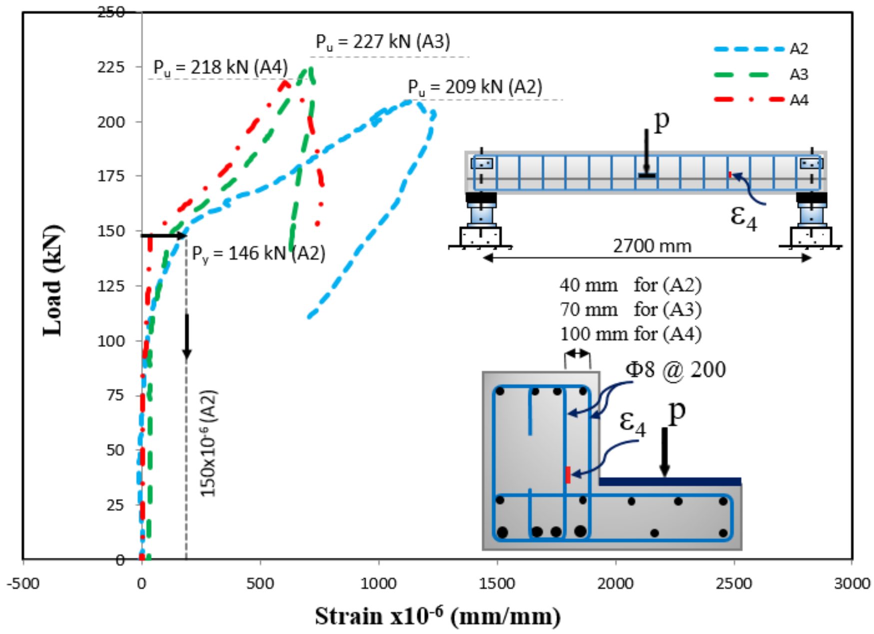

Figure (18): Load versus strains of inner stirrups (□□) at quad-span of beams A1 to A4

4. NUMERICAL ANALYSIS

The main aim of performing a finite element analysis of the models was to extend the investigations carried out experimentally to have better understanding of the behavior of all tested ledge RC beams.

4.1. Model Description

A finite element model was performed to simulate the joints in the realistic way using program ABAQUS/CAE V6.9. The specimens were modeled with the same dimensions performed in the tests. The concrete core was modeled using solid element called C3D8R, which is an eight-node linear brick with an element size of 25 mm. For the internally reinforced specimens, the rebars were modeled using T3D2. The loading was applied as a concentrated load at one node on the loading plate. The static riks procedure was used as the chosen solution strategy. The geometric non linearity was considered in the analysis in order to account for the second order effects.

4.2. Modeling of Material Properties

The concrete was modeled using the concrete smeared cracking option available in the ABAQUS finite element program. Concrete compression hardening was defined using the true stress- plastic strain relation as described in ABAQUS documentation. Young's modulus for concrete E_c was defined using the ACI formulation and poisons ratio was taken 0.2. Elastic and Plastic material options are used for defining steel reinforcement as elastic-perfectly plastic materials. The yield, ultimate strengths and ultimate strain for the steel reinforcement were defined according to the tension coupons test results. The elastic properties were defined as 200000 MPa for young's modulus and 0.3 for the Poisson ratio.

4.3. Results and Verification of FE Models

Table 5 shows the hanger and punching failure load obtained from the experimental program and the corresponding FEM predictions for the beams, moreover it gives the ratio between the FE and the experimental results for the hanger and punching failure loads. The results show that the average deviation between the FE and experimental results for hanger failure loads was in a range of 2.17 % with standard deviation of 1.22 % and for punching failure loads was in a range of 2.47 % with standard deviation of 3.53 %, as shown in Table 5. In addition, Figure 19 and 20 show a comparison between the experimental and FE results in terms of steel hanger failure loads and punching failure loads for all beams.

Table (5): Comparison between the experimental and numerical results.

Specimen	Hanger failure load (kN)		Hanger failure load % (F.E. / Exp.)	Punching failure load (kN)		Punching failure load % (F.E. / Exp.)
	F.E.	Exp.		F.E.	Exp.	
A1	124	125	99.20	204	197	103.55
A2	140	146	95.89	225	209	107.66
A3	132	135	97.78	223	227	98.24
A4	127	129	98.45	219	218	100.46
Average			97.83	Average		102.47
Standard deviation			1.22	Standard deviation		3.53

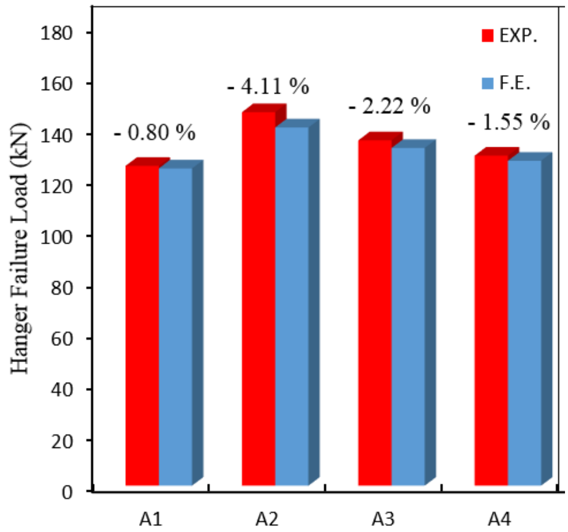

Figure (19): Experimental versus F.E. in terms of hanger failure loads.

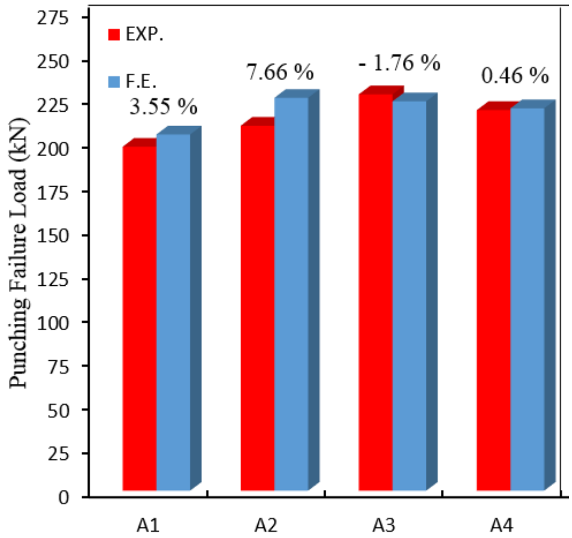

Figure (20): Experimental versus F.E. in terms of punching failure loads.

5. CONCLUSIONS

The findings of this study have shown that the inner stirrups can effectively be used as a steel hanger reinforcement to reduce the outer vertical stirrups amount. The following main conclusions as follows:

1- The use of inner stirrups reinforcement has a considerable effect on the hanger load capacity of ledge beams. The experimental results showed that the hanger load capacity was increased by 17 % with using inner stirrups spaced 40 mm measured from the outer stirrups compared with the ledge beam with outer stirrups only whereas it was increased by 8 % and 3 % with using inner stirrups spaced 70 mm and 100 mm measured from the outer stirrups, respectively.

2- The effective width which the hanger reinforcement transfer the vertical load acting on the ledge part in case of using outer stirrups only is (5 - 6) times the ledge beam depth each side from the acting load. This is in good agreement with The PCI Handbook [9] and it deviates clearly from the values proposed in the PCA notes on ACI code [1].

3- The effective width which the hanger reinforcement transfer the vertical load acting on the ledge part in case of using inner stirrups is (0.40 – 1.20) times the ledge beam depth each side from the acting load.

4- The concept of adding the area of hanger steel reinforcement to the reinforcement resisting shear and torsion stresses according to the PCA notes on ACI code [1] leads to overestimating the required transverse reinforcement. According to the PCI Handbook [9], the greater amount of the two terms (hanger or shear & torsion reinforcement) should be chosen. The later approach is in a good agreement with the experimental and numerical results.

5- The obtained results shows that the PCI Handbook [9] is underestimated the punching shear strength of ledge beams, while it can be estimated according to the PCA notes on ACI code [1] with a good accuracy.

6. REFERENCES

[1] ACI Committee 318 (2014). ACI 318-14: Building Code Requirements for Structural Concrete and Commentary.

[2] Mostafa, Ezz, (2015). Effect of Hanger Steel Reinforcement and Its Location on the Behavior of Ledge Beam (PHD Thesis, faculty of engineering, Ain Shams University).

[3] Hasan, T. (2007). Finite Element Study of Shear Behavior of Spandrel Ledges and Comparison with PCI Shear Design Provisions. Advances in Structural Engineering 10, 475–485.

[4] Hasan, T., Lucier, G., Rizkalla, S., and Zia, P. (2007). Modeling of L-shaped, precast, prestressed concrete spandrels. PCI Journal 52, 78-92.

[5] Klein, G.J. (1986a). Design of Spandrel Beams. PCI Journal 31, 76–124.

[6] Logan, D. R. (2012). "Development of a Rational Design Methodology for Precast Slender Spandrel Beams." PCI Journal 57, 182–187.

[7] Lucier, G., Walter, C., Rizkalla, S., Zia, P., and Klein, G. (2010). Development of a Rational Design Methodology for Precast Slender Spandrel Beams. North Carolina State University (Report).

[8] Lucier, G., Walter, C., Rizkalla, S., Zia, P., and Klein, G. (2011a). Development of a Rational Design Methodology for Precast Concrete Slender Spandrel Beams: Part 1, Experimental Results. PCI Journal 56, No. 2 (spring), 88–112.

[9] Precast/Prestressed Concrete Institute (2010). PCI Design Handbook 7th Edition.

[10] Badawy, Yasser ” Contribution of Inner Stirrups with the Hanger Steel Reinforcement on the Behaviour of Ledge Beam” PhD Thesis, Ain Shams University, 2017 (under publication)